eNeurologicalSci 22 (2021) 100310

Contents lists available at ScienceDirect

eNeurologicalSci

journal homepage: www.elsevier.com/locate/ensci

Pathologic basis of the preferential thinning of thecorpus callosum in adult-onset leukoencephalopathy with axonal spheroids and pigmented glia (ALSP)

Michiaki Kinoshita [a], Kiyomitsu Oyanagi [b,*], Yasufumi Kondo [c], Keisuke Ishizawa [d], Kenji Ishihara [e], Mari Yoshida [f], Teruhiko Inoue [g], Yoshio Mitsuyama [g], Kunihiro Yoshida [h], Mitsunori Yamada [b], Yoshiki Sekijima [c], Shu-ichi Ikeda [i]

[a] Department of Neurology, Suwa Red Cross Hospital, 5-11-50 Kogandori, Suwa 392-8510, Japan
[b] Division of Neuropathology, Department of Brain Disease Research, Shinshu University School of Medicine, 3-1-1 Asahi, Matsumoto 390-8621, Japan
[c] Department of Medicine (Neurology and Rheumatology), Shinshu University School of Medicine, 3-1-1 Asahi, Matsumoto 390-8621, Japan
[d] Departments of Neurology and Pathology, Saitama Medical University, 38 Morohongo, Moroyama-machi, Iruma-gun, Saitama 350-0495, Japan
[e] Department of Internal Medicine, Ushioda General Hospital, 1-6-20 Yako, Tsurumi-ku, Yokohama 230-0001, Japan
[f] Department of Neuropathology, Institute for Medical Science of Aging, Aichi Medical University, 1-1 Yazakokarimata, Nagakute, 480-1195, Japan
[g] Psychogeriatric Center, Daigo Hospital, 1270 Nagata, Mimata-chou, Kitamorokata-gun, Miyazaki 889-1911, Japan
[h] Division of Neurogenetics, Department of Brain Disease Research, Shinshu University School of Medicine, 3-1-1 Asahi, Matsumoto 390-8621, Japan
[i] Intractable Disease Care Center, Shinshu University Hospital, 3-1-1 Asahi, Matsumoto 390-8621, Japan

ARTICLE INFO

Keywords:
ALSP
Corpus callosum
CSF1R
HDLS
Lesion staging
Microglia

ABSTRACT

Background: Adult-onset leukoencephalopathy with axonal spheroids and pigmented glia (ALSP) is an early onset dementia characterized by axonal loss in the cerebral white matter with swollen axons (spheroids). It had been reported that the preferential thinning and "focal lesions" of the corpus callosum were observed on T2-weighted MRI in ALSP patients. The present study aimed to reveal the pathologic basis of them in relation to brain lesion staging (I ~ IV: Oyanagi et al. 2017).
Methods: Seven autopsied brains of ALSP and five controls were neuropathologically examined.
Results: Even at Stage I, corpus callosum body showed evident atrophy, and the atrophy advanced with stage progression. Spheroid size and density were maximal at Stage II in both centrum semiovale and corpus callosum body, but spheroids were larger in corpus callosum body than in centrum semiovale. Microglia in the body at Stage II had a larger cytoplasm than those in centrum semiovale. But spheroids and microglia in the "focal lesions" were identical with those of centrum semiovale.
Conclusion: Preferential thinning of corpus callosum was considered to be formed in relation to peculiar morphological alteration of microglia there in ALSP. Instead, "focal lesions" were formed in connection with the lesions in centrum semiovale.

1. Introduction

Among the hereditary leukoencephalopathies causing early onset dementia, adult-onset leukoencephalopathy with axonal spheroids and pigmented glia (ALSP)/hereditary diffuse leukoencephalopathy with axonal spheroids (HDLS) is an autosomal-dominant cerebral white matter disease characterized by axonal loss with swollen axons (spheroids) and marked alteration of microglia, astrocytes and oligodendroglia in the lesions [1–15]. The colony stimulating factor 1 receptor gene (*CSF1R*) [8,16–18] and the alanyl-transfer (t)RNA synthetase 2 (*AARS2*)

* Corresponding author at: Division of Neuropathology, Department of Brain Disease Research, Shinshu University School of Medicine, 3-1-1 Asahi, Matsumoto 390-8621, Japan.
E-mail addresses: mkinoshi@shinshu-u.ac.jp (M. Kinoshita), k123ysm@shinshu-u.ac.jp (K. Oyanagi), gingnang@shinshu-u.ac.jp (Y. Kondo), ishik.kishi@gmail.com (K. Ishizawa), ishiharakenji@hotmail.com (K. Ishihara), myoshida@aichi-med-u.ac.jp (M. Yoshida), inoue@fujimoto.or.jp (T. Inoue), mitsuyama@fujimoto.or.jp (Y. Mitsuyama), kyoshida@shinshu-u.ac.jp (K. Yoshida), nori@shinshu-u.ac.jp (M. Yamada), sekijima@shinshu-u.ac.jp (Y. Sekijima), ikedasi@shinshu-u.ac.jp (S.-i. Ikeda).

https://doi.org/10.1016/j.ensci.2021.100310
Received 31 July 2020; Received in revised form 2 December 2020; Accepted 31 December 2020
Available online 22 January 2021

gene [19–22] have been implicated as causative genes of ALSP. CSF1R is expressed mainly in microglia [23], which are thought to play an important role in the pathogenesis of white matter degeneration in ALSP [1,8,11,17,18,24,25]. *AARS2* encodes a mitochondrial enzyme, and its mutation has recently been reported to cause a leukoencephalopathy showing clinical and pathological features identical to those of ALSP attributable to *CSF1R* mutation [19–22].

Brain imaging has demonstrated marked atrophy of the corpus callosum even at the early stage of ALSP [4,12,26–30]. Using quantitative determination of corpus callosum thickness (corpus callosum index: CCI) demonstrated by midsagittal MRI [31,32], the present authors have shown that this corpus callosum atrophy is significant in ALSP and occurs early in the disease course [26]. However, the pathological features of the corpus callosum in ALSP, particularly those of "focal corpus callosum lesions" that are frequently demonstrable by high-intensity T2-weighted MRI [18,27,29,30,33–35], have not yet been reported in detail and the mechanism has not been elucidated.

Many autopsy reports have macroscopically pointed a marked thinning of the corpus callosum in patients with ALSP, and only two papers reported the histological findings of the corpus callosum [25,36], however, chronological alteration of the histopathological findings of the corpus callosum along with the progression of the brain lesion staging and the pathologic basis of those findings of the corpus callosum have not been reported and the mechanism of the thinning is still unknown. The present study aimed to clarify the detailed neuropathological features of the corpus callosum in ALSP and the mechanism, by focusing especially on 1) the features in microglial alteration compared with those in centrum semiovale, 2) the "focal corpus callosum lesions" revealed by MRI, and 3) pathologic basis of the preferential thinning of the corpus callosum.

2. Materials and methods

2.1. Examined cases

All of the patients examined in the present study, except for #3 [37], were the same as those documented in our recent previous investigation [1]. We examined seven autopsied brains of ALSP patients from five families (four males and three females; ages at autopsy 41–58 years; mean age ± standard deviation 51.86 ± 6.67 years) [8,10,24,26,27,36–38]. All of the patients were Japanese, and mutations in *CSF1R* were identified in six of them. The remaining patient was diagnosed as having ALSP on the basis of clinical and neuropathological findings [37]. *AARS2* genes status was not examined in any of the patients. Table 1 shows the characteristics of the seven ALSP patients, including their family lines, gene mutations, sex, age at onset, age at death, clinical symptoms and the modified Rankin scale (mRS) [39] at death, brain weight and thickness of the corpus callosum.

The brain lesions of ALSP were staged according to Oyanagi et al. (2017) as follows [1]. Stage I, patchy axon loss in the cerebral white matter without brain atrophy; Stage II, large patchy areas of axon loss with slight atrophy of the cerebral white matter and slight dilatation of the lateral ventricles; Stage III, extensive axon loss in the cerebral white matter and dilatation of the lateral and third ventricles without marked axon loss in the brainstem and cerebellum; Stage IV, cerebral white matter destruction with marked dilatation of the ventricles and axon loss in the brainstem and/or cerebellum.

Patient #1 was at Stage I, patients #2 and #3 were at Stage II, patients #4, #5 and #6 were at Stage III, and patient #7was at Stage IV. Five controls (three males and two females; ages at autopsy 62–76 years; mean age ± standard deviation 69.4 ± 5.03 years), who had also been used in our previous study [1], were included for comparison of the neuropathological features.

2.2. Neuropathological procedures

Formalin-fixed paraffin-embedded 6-μm-thick coronal sections of the corpus callosum and centrum semiovale from these seven autopsied brains were subjected to neuropathological examination with hematoxylin and eosin (HE) and Klüver-Barrera (K-B) staining, as well as immunohistochemistry for phosphorylated (p)-neurofilament (NF), Iba-1 (ionized calcium binding molecule-1) which has been reported to be a

Table 1
Clinical characteristics, brain weights and thickness values of corpus callosum in ALSP patients.

Patient	#1	#2	#3	#4	#5	#6	#7
Stage (Oyanagi et al. 2017) [1]	I	II	II	III	III	III	IV
Family line	AI1	SH1	ST	YK	MY1	MY1	MY1
CSF1R gene mutation	p. C653Y	p. K793T	−	p. S688EFsX13	p. I794T	p. I794T	p. I794T
Sex	F	M	F	F	M	M	M
Age at onset (years)	no symptoms	40	56	41	40	52	40
Age at death (years)	44	41	57	54	56	58	53
Duration of disease (years)	−	1	1	13	16	6	13
Family history	+	−	−	−	+	+	+
Brain weight (g)	1330	1430	1320	910	980	1010	1000
Thickness of CC at body level (mm)	3.287	2.129	3.400	1.342	0.601	0.594	0.566
Neuropsychiatric symptoms							
Cognitive decline	−	+	+	+	+	+	+
Depression/Anxiety	−	+	−	−	+	−	nd
Behavioral change	−	+	+	+	nd	+	+
Frontal releasing	−	+	+	+	+	+	+
Pyramidal tract signs	−	−	+	−	nd	+	nd
Parkinsonism	−	+	nd	−	nd	nd	+
Epilepsy	−	−	−	−	+	−	+
mRS at death	0	3	5	5	5	5	5
References	[1,10,24]	[1,26,27,38]	[37]	[1,8,25,36]	[1]	[1]	[1]

Patients examined in the present study except for #3 [37] were the same as those in the previous study by Oyanagi et al. (2017) [1]. Patient #1, whose sister suffered from ALSP diagnosed by gene and neuropathological examination, had no neuropsychiatric symptoms during her life, but the autopsied brain showed leukoencephalopathy with spheroids [1,10,24]. Patient #2 had been diagnosed on the basis of genetic examination when mild cognitive disturbance appeared [26,27,38]. He died of sepsis unexpectedly in the early stage of the disease. Patient #3 was diagnosed as having ALSP by neuropathological examination [37], but did not carry any mutation in *CSF1R*, triggering receptor expressed on myeloid cells 2 (*TREM2*) or DNAX-activating protein 12 (*DAP12*), which are causative genes of Nasu-Hakola disease [54,55]. Patient #4 showed marked brain atrophy. Patients #5, #6 and #7 were cousins. *CSF1R* p. I794T had been recently detected in this family (personal communication to YM, one of the present authors). The lesion staging reported by Oyanagi et al. was adopted (Fig. 1) [1]. Abbreviations: CC; corpus callosum, M; male, F; female, nd; not described, mRS; modified Rankin scale [39].

microglia-specific calcium binding protein [40,41], cluster of differentiation (CD) 68 which is a marker of phagocytic function, being localized in lysosomes [42], and CD163 which is a marker of macrophage/monocyte/microglia, being a hemoglobin scavenger receptor related to macrophage activation [42,43]. The corpus callosum was examined at the body level in all patients, and also at the splenium level in patient #2.

Thickness of the corpus callosum was measured at the smallest parts of the body level square with the K-B stained corpus callosum in the patients and five controls using Cell Sence™ software (Olympus, Tokyo, Japan).

Immunohistochemical staining was performed using the avidin-biotin-peroxidase complex (ABC) method (Vectastain ABC Elite kit, Vector, Burlingame, CA, USA). Non-specific binding of the ABC system reagents was blocked by pretreating the sections with 0.3% hydrogen peroxide in methanol and normal blocking serum, and then incubating them with the required primary antibody overnight at 4 °C. The sections were then rinsed in phosphate-buffered saline with Triton X-100 (PBST) and incubated for 1 h with the secondary reagent containing a biotinylated anti-rabbit or anti-mouse IgG antibody (diluted 1:200) at 37 °C, and finally with the ABC solution for 1 h at room temperature (RT). The sections were subjected to a peroxidase reaction with 30 μL ImmPACT™ DAB Chromogen Concentrate (Vector) (diluted 1:2, with 50 mmol/L Tris HCL (pH 7.6)) in 1 mL ImmPACT™ Diluent (Vector) at RT. After stopping the reaction, the sections were rinsed in tap water, then stained with hematoxylin.

For CD68 and p-NF, antigenicity for immunohistochemistry was increased by boiling the sections in 0.01 mol/L citrate-buffered solution (pH 7.6) in a microwave oven (750 W, 25 min), and for Iba-1 and CD163 by autoclaving (121 °C, 20 min) in 0.01 mol/L citrate-buffered solution (pH 6.0). Primary antibodies used for immunohistochemistry are listed in Table 2.

Some of the sections of the corpus callosum and centrum semiovale were subjected to double staining with periodic acid-Schiff (PAS) and immunohistochemistry for p-NF, and double immunohistochemistry for CD163 with IBA-1. The sections were processed by autoclaving, and then treated with anti-CD163 antibody (1:100), followed by staining with Vectastain Blue (Vector). The anti-Iba-1 antibody (1:2000) was then applied, and the sections were subjected to the peroxidase reaction.

As antibody controls, the primary antisera were either omitted or replaced with normal rabbit or mouse serum. Several specimens of neural and non-neural tissue from the patients served as positive or negative tissue controls.

The density and diameter of axons and spheroids, and the density, size and changes in the features of the cells immunopositive for p-NF, IBA-1, CD163 and CD68 were compared between the corpus callosum and centrum semiovale.

Table 2
Antibodies used.

Detection	Antibody type	Dilution	Increase of antigenicity	Source
Phosphorylated neurofilament	Mouse/ monoclonal (clone SMI31)	1:2000	Boiling	COVANCE, Princeton, USA
IBA-1	Rabbit/ polyclonal	1:4000	Autoclaving	Wako Pure Chemical Industries, Osaka, Japan
CD163	Mouse/ monoclonal (clone 10D6)	1:200	Autoclaving	Leica Biosystems, Newcastle Upon Tyne, UK
CD68	Mouse/ monoclonal (clone KP1)	1:800	Boiling	DAKO, Glostrup, Denmark

Antigenicity was increased by autoclaving (121° C, 20 min) in 0.01 mol/L citrate-buffered solution (pH 6.0) for Iba-1 and CD163. Boiling in a microwave oven (500 W, 7 min) in 0.01 mol/L citrate-buffered solution (pH 7.6) for phosphorylated neurofilament and CD68.

3. Results

3.1. Corpus callosum thickness

The thickness of the corpus callosum measured at the smallest parts of the body level was 3.475 ± 0.456 (mean ± SD) mm in the controls. As for the ALSP cases, the thickness of the corpus callosum at the body level was reduced even at Stage I, and thinning advanced with stage progression (Table 1, Fig. 1). "Focal lesion" at the corpus callosum splenium (Fig. 1C, arrowhead) connected with the lesions in the centrum semiovale (Fig. 1C).

3.2. Axon loss and spherically swollen axons (spheroids)

Axonal or myelinated fiber density in the lesions of the centrum semiovale was slightly and patchily decreased at Stage I (Figs. 2A, 3A), reduced in the lesions at Stage II (Figs. 2C, 3C), and extensive destruction was evident at Stages III (Figs. 2G, 3G) and IV (Figs. 2I, 3I). However, the density in the corpus callosum body appeared to be preserved due to compaction at Stage I (Figs. 2B, 3B), and decreased with disease progression from Stage II, although better preservation was evident relative to the centrum semiovale (Figs. 2C, D, G, H, I, J, 3C, D, G, H, I, J). The ventral half of the corpus callosum splenium showed moderate loss of axons in Patient #2 at Stage II (Figs. 2F, 3F), and the dorsal half of the splenium, corresponding to the "focal lesions" evident on MRI, showed loss of axons (Figs. 2E, 3E) (Table 3).

Spheroids with a maximal diameter of 20 μm were scattered in the lesions in the centrum semiovale (Fig. 3A) and the body of the corpus callosum (Fig. 3B) at Stage I, and those with a maximal diameter of 40 μm were observed extensively in the lesions in the centrum semiovale (Fig. 3C), and in the body (Fig. 3D) and dorsal part of the splenium (Fig. 3E) of the corpus callosum in Patient #2 at Stage II, although spheroids in the ventral part of the splenium were less than 20 μm in diameter at this stage (Fig. 3F). A few spheroids with a maximum diameter of 15 μm were present in the centrum semiovale (Fig. 3G) and body of the corpus callosum (Fig. 3H) at Stage III, and in the centrum semiovale (Fig. 3I) at Stage IV, but scarcely observed in the body of the corpus callosum (Fig. 3J) at Stage IV (Table 3).

No calcium deposition was observed in the portions examined.

3.3. Iba-1-immunopositive microglial cells

Many ramified cells with long and thin processes, whose cytoplasmic diameters were less than 10 μm, were seen in the centrum semiovale (Fig. 4A) and body of the corpus callosum (Fig. 4B) at Stage I (Table 4). On the other hand, rounded cells with a maximal cytoplasmic diameter of 25 μm and short, thick processes were abundant in the centrum semiovale (Fig. 4C) and dorsal part of the corpus callosum splenium (Fig. 4E) in Patient #2 at Stage II, corresponding to the "focal lesions" revealed by MRI. Round amoeboid cells with maximal diameter of 25 μm without remarkable cell processes were present in the body of the corpus callosum (Fig. 4D), whereas cells with thick processes were evident in the ventral part of the splenium (Fig. 4F) in Patient #2 at Stage II (Table 4). Oval amoeboid cells without evident cell processes, whose cytoplasmic diameters were maximally 15 μm, were seen in the centrum semiovale (Fig. 4G), and amoeboid cells with a maximal cytoplasmic diameter of 20 μm were observed in the body of the corpus callosum (Fig. 4H) at Stage III (Table 4). Scattered small ramified cells with a cytoplasmic diameter less than 10 μm were seen in both the corpus callosum body (Fig. 4I) and centrum semiovale (Fig. 4J) at Stage IV (Table 4).

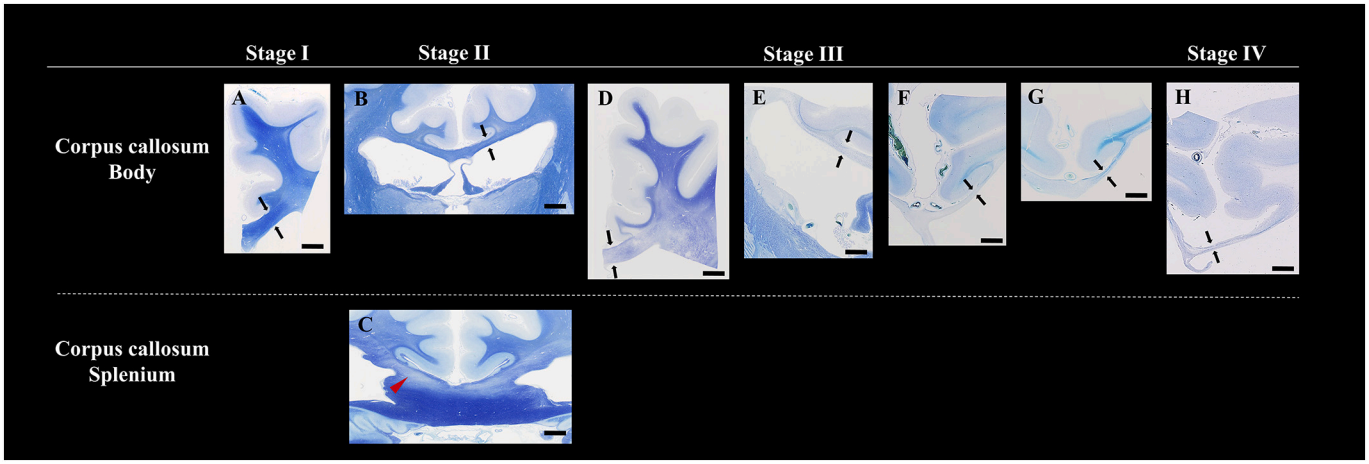

Fig. 1. Coronal sections of the corpus callosum at each ALSP lesion stage.
A; patient #1 at Stage I, B, C; patient #2 and D; Patient #3 at Stage II, E; patient #4, F; patient #5 and G; patient #6 at Stage III, and H; patient #7 at Stage IV. No remarkable paleness was observed in the corpus callosum or centrum semiovale in the control brains (data not shown). Paleness of myelin staining and atrophy was exacerbated with disease progression in the body of the corpus callosum of patients with ALSP. Thickness of the corpus callosum at the body level was measured at the smallest parts square with the corpus callosum between the arrows in each patient (A - H). Thickness of the corpus callosum is shown in Table 1. Red arrowhead shows the lesion in the dorsal part of the splenium in patient #2 at Stage II (C), which corresponds to the "focal corpus callosum lesion" revealed by MRI, connecting with the centrum semiovale lesions. Klüver-Barrera (K-B) preparation. Bars; 5 mm at Stages I and II (A-D); 10 mm at Stages III and IV (E-H). (For interpretation of the references to colour in this figure legend, the reader is referred to the web version of this article.)

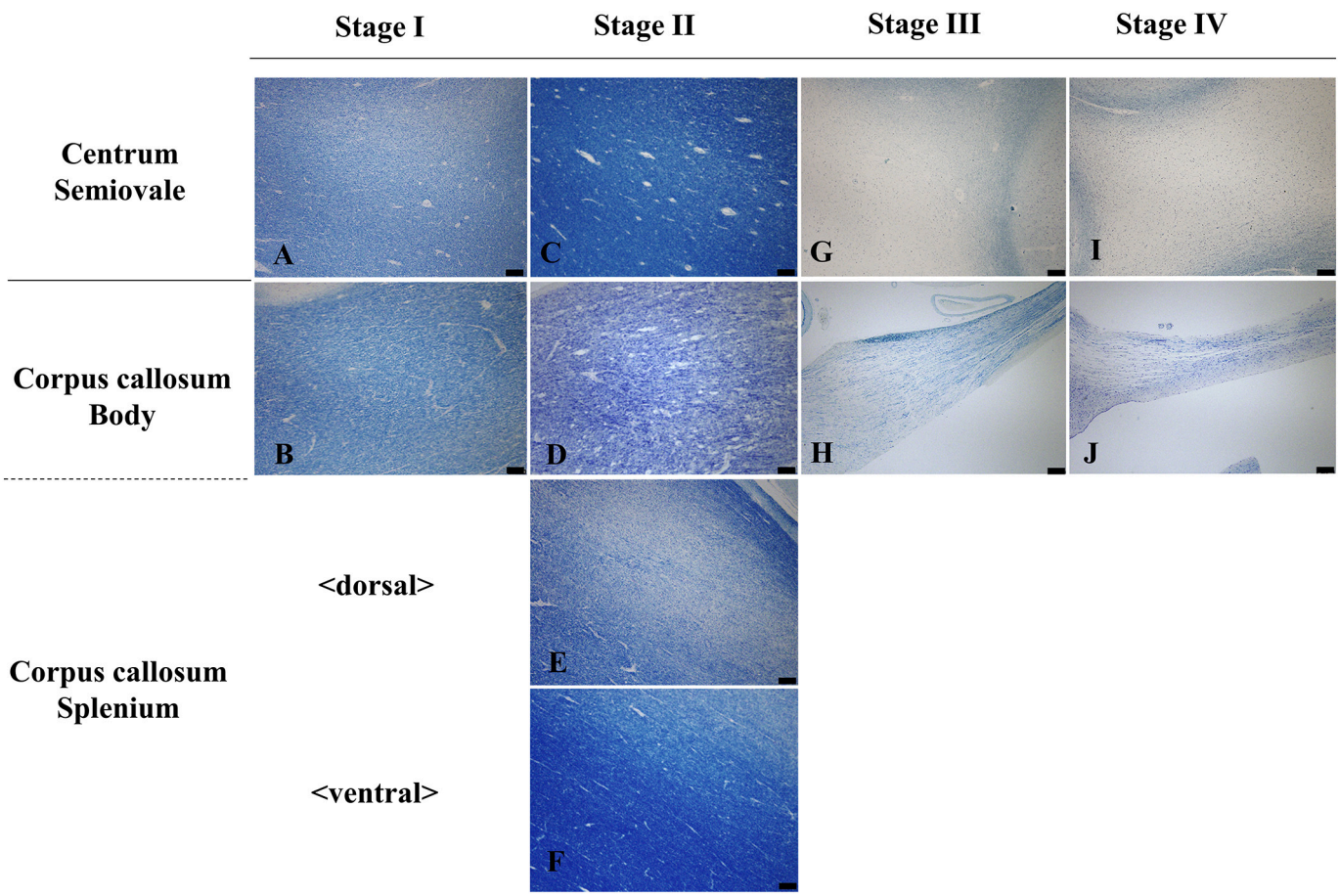

Fig. 2. Loss of myelinated fibers in the centrum semiovale and corpus callosum.
Paleness of myelin staining was exacerbated with disease progression in the body of the corpus callosum (B, D, H, J) and centrum semiovale (A, C, G, I). The dorsal part of the corpus callosum in Patient #2 at Stage II, corresponding to the "focal lesions" revealed by MRI, showed severe paleness (E) as compared with the ventral part (F). Klüver-Barrera (K-B) preparation. Bars; 200 μm.

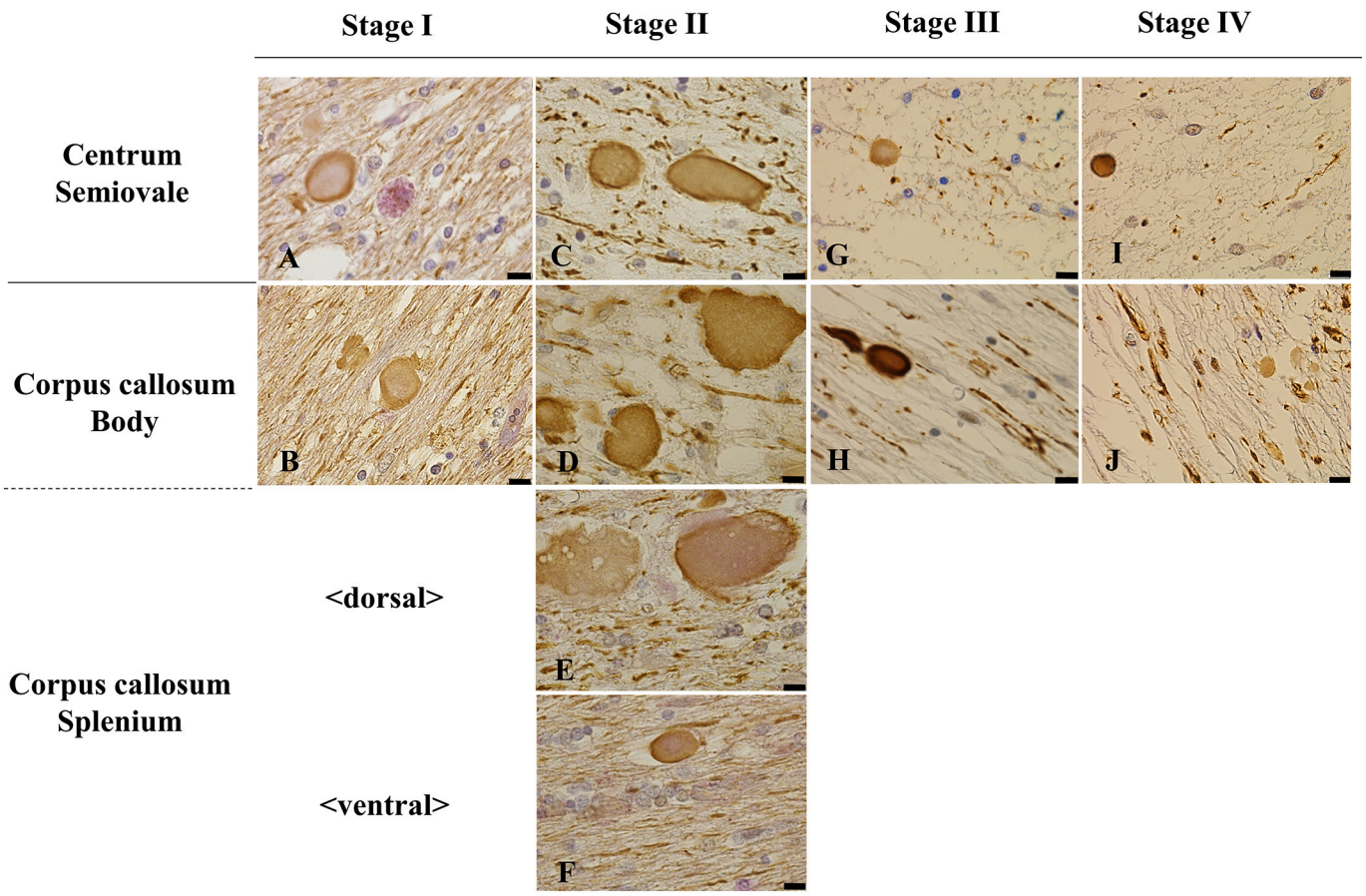

Fig. 3. Axonal changes.
No significant axon loss or spheroids were observed in the corpus callosum and centrum semiovale in the control brains (data not shown). Axonal density was slightly and patchily sparse in the centrum semiovale at Stage I (A), markedly reduced at Stage II (C), and extensive destruction was evident at Stages III (G) and IV (I). Axonal density in the corpus callosum body decreased slightly at Stage I (B), and reduced severely at Stages II (D), III (H) and IV (J). But the severity was slighter than that of centrum semiovale due to compaction of axons in the corpus callosum. The dorsal half of the splenium in Patient #2 at Stage II, corresponding to the "focal lesions" evident on MRI, showed marked loss of axons (E), whereas axons in the ventral half were relatively preserved (F).
Spheroids with a maximal diameter of 20 μm were scattered in the centrum semiovale (A) and the body of the corpus callosum (B) at Stage I, and those with a maximal diameter of 40 μm were abundant in the centrum semiovale (C), and the body (D) and dorsal part of the splenium (E) of the corpus callosum in Patient #2 at Stage II. But the size of the spheroids in the corpus callosum body and in the dorsal part of the splenium is relatively larger than that in the centrum semiovale at Stage II and largest as compared with that in other stages. Spheroids in the ventral part of the splenium were less than 20 μm in diameter at Stage II (F). A few spheroids with a maximum diameter of 15 μm were present in the centrum semiovale (G) and body of the corpus callosum (H) at Stage III, and in the centrum semiovale at Stage IV (I), but were scarcely evident in the corpus callosum body at Stage IV (J).
No calcium deposition was observed in any of the portions examined. Immunohistochemistry for phosphorylated (p-) neurofilament (NF) (SMI-31) (C, D, and G-J). Double staining using periodic acid-Schiff (PAS) and immunohistochemistry for p-NF (A, B, E and F). Bars; 10 μm.

Table 3
Axonal loss and swollen axons.

Patient	#1	#2	#3	#4	#5	#6	#7
Stage (Oyanagi et al. 2017) [1]	I	II	II	III	III	III	IV
Axonal loss							
Centrum Semiovale	patchy	diffuse	diffuse	extensive	extensive	extensive	extensive
Corpus Callosum Body	slight	diffuse	diffuse	extensive	extensive	extensive	extensive
Splenium <dorsal>		diffuse					
Splenium <ventral>		slight					
Swollen axons							
Centrum Semiovale	20 μm maximal, scattered	40 μm maximal, many	40 μm maximal, many	15 μm maximal, a few	15 μm maximal, a few	15 μm maximal, a few	15 μm maximal, a few
Corpus Callosum Body	20 μm maximal, scattered	40 μm maximal, many	40 μm maximal, many	15 μm maximal, a few	15 μm maximal, a few	10 μm maximal, few	10 μm maximal, few
Splenium <dorsal>		40 μm maximal, many					
Splenium <ventral>		20 μm maximal, scattered					

Semiquantitative evaluation of the findings of immunohistochemistry for phosphorylated (p-) neurofilament (NF) (SMI-31) of all the patients. The numbers indicate diameters of swollen axons (spheroids).

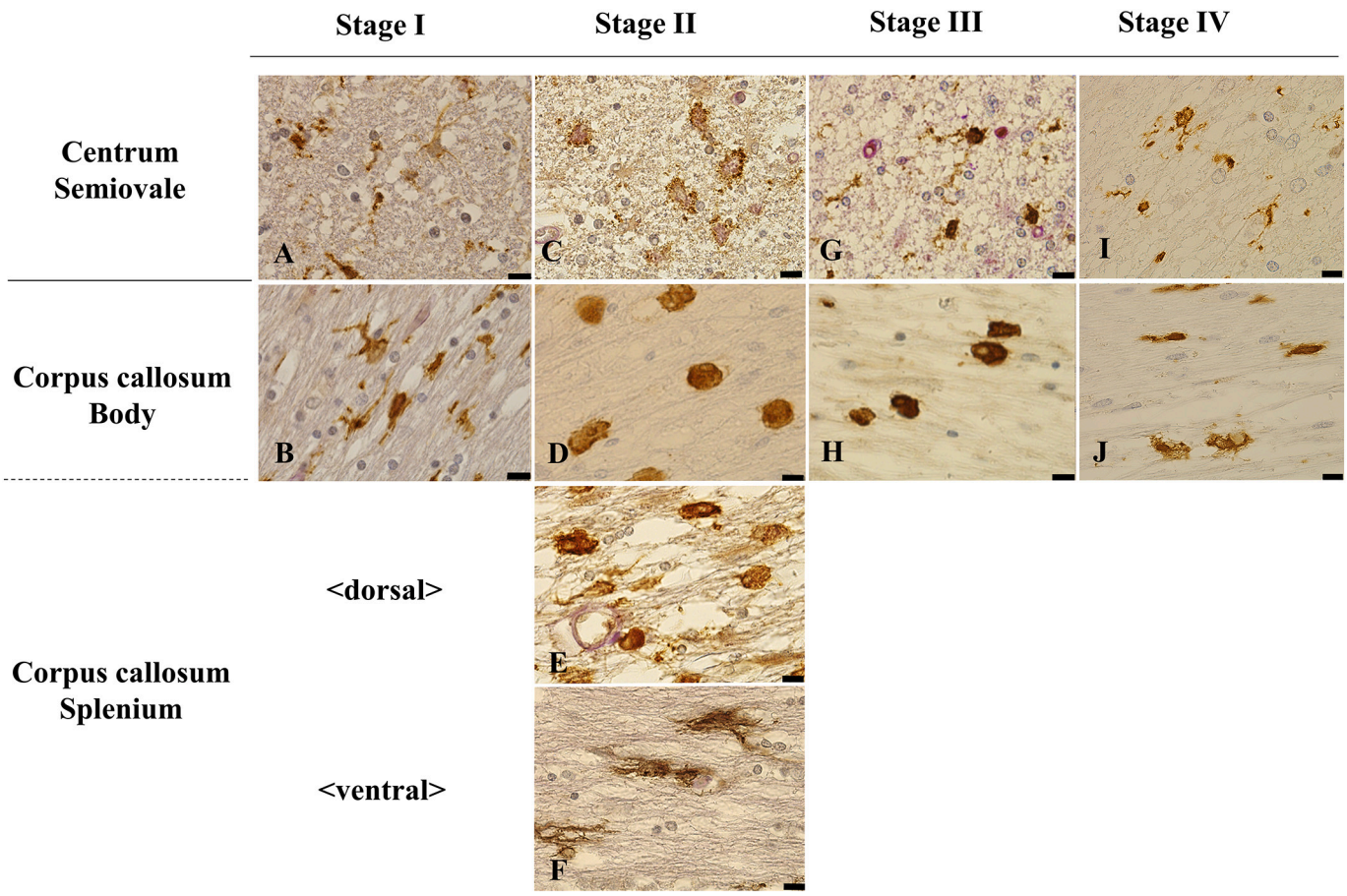

Fig. 4. Iba-1-immunopositive microglial cells.
Many ramified cells with long, thin processes and soma less than 10 μm in diameter were present in the centrum semiovale (A) and body of the corpus callosum (B) at Stage I. On the other hand, round cells with maximal cytoplasmic diameter of 25 μm with short and thick processes were abundant in the centrum semiovale (C) and dorsal part of the splenium (E) in Patient #2 at Stage II, corresponding to the "focal lesions" revealed by MRI, whereas round cells without remarkable cell processes were present in the body of the corpus callosum (D), and cells sizing maximal diameter of 20 μm with thick processes were evident at the ventral part of the splenium (F) in Patient #2 at Stage II. Oval amoeboid cells without remarkable cell processes were present in the centrum semiovale (G) and the corpus callosum body (H) with maximal cytoplasmic diameters of 15 μm and 20 μm at Stage III, respectively. Scattered small ramified cells less than 10 μm were seen in both the corpus callosum (I) and centrum semiovale (J) at Stage IV. Iba-1 immunohistochemistry (brown) (D, I and J). Double staining using periodic acid-Schiff (PAS) and immunohistochemistry for Iba-1 (brown) (A - C, and E - H). Bars; 10 μm. (For interpretation of the references to colour in this figure legend, the reader is referred to the web version of this article.)

3.4. *CD163-immunopositive microglial cells*

Amoeboid cells with a maximal cytoplasmic diameter of 15 μm and a few short processes were scattered in both the centrum semiovale (Fig. 5A) and corpus callosum body (Fig. 5B) at Stage I (Table 4). Polygonal cells with a maximal cytoplasmic diameter of 20 μm, possessing several thick short processes, were abundant in the centrum semiovale (blue in Fig. 5C) and dorsal (blue in Fig. 5E) and ventral (blue in Fig. 5F) parts of the splenium in Patient #2, whereas oval amoeboid cells with a maximal diameter of 20 μm were scattered in the body of the corpus callosum at Stage II (Fig. 5D) (Table 4). A few or less small oval or polygonal cells with a diameter of less than 10 μm and sparse processes were present in the centrum semiovale and body of the corpus callosum at Stages III and IV (Figs. 5G - 5 J) (Table 4).

3.5. *CD68-immunopositive microglial cells*

Oval-shaped amoeboid cells with a maximal cytoplasmic diameter of 20 μm were scattered in both the centrum semiovale (Fig. 6A) and corpus callosum body (Fig. 6B) at Stage I (Table 4). Many of these cells were present in the centrum semiovale (Fig. 6C), the body level (Fig. 6D) and the dorsal part of the corpus callosum splenium (Fig. 6E) in Patient #2 at Stage II, corresponding to the "focal lesions" revealed by MRI, but few were evident in the ventral part of the splenium (Fig. 6F) (Table 4). A few cells less than 10 μm in diameter were seen in the centrum semiovale and body of the corpus callosum at Stages III and IV (Figs. 6G - 6 J) (Table 4).

4. Discussion

Microglia have been classified morphologically into ramified and amoeboid types. Ramified microglia have long, thin and branched processes and are regarded as a "resting type" [44], whereas round or oval-shaped amoeboid microglia have short and thick processes and are considered to be an "activating type" [45]. Activating microglia are thought to be induced by certain cytokines, such as interleukin-34 (IL-34), which act via CFS1R after being secreted from damaged neurons in the brain [46–48].

Several reports have been published pointing the specificity of the microglia and of the pathological peculiarity of the corpus callosum. Cuprizone induced demyelination and increase of microglia specifically in the corpus callosum [49], one-year-old *Csf1r*+/− mice revealed thinning of the corpus callosum [50], and an individual human with a homozygous splice mutation (c.1754_1G > C) in *CSF1R* demonstrated

Table 4
Evaluation of microglial alteration.

Patient	#1	#2	#3	#4	#5	#6	#7
Stage (Oyanagi et al. 2017) [1]	I	II	II	III	III	III	IV
Iba-1							
Centrum Semiovale	ramified, less than 10 μm, many	large round with short processes, 25 μm maximal, many	large round with short processes, 25 μm maximal, many	small ramified, 15 μm maximal, scattered	small ramified, 15 μm maximal, scattered	small ramified, 15 μm maximal, scattered	small ramified, less than 10 μm, scattered
Corpus Callosum Body	ramified, less than 10 μm, many	large amoeboid, 25 μm maximal, many	large amoeboid, 25 μm maximal, many	amoeboid, 20 μm maximal, scattered	amoeboid, 20 μm maximal, scattered	small amoeboid, less than 10 μm, scattered	small ramified, less than 10 μm, scattered
Splenium <dorsal>		large round with short processes, 25 μm maximal, many					
Splenium <ventral>		large ramified, 20 μm maximal, many					
CD163							
Centrum Semiovale	small amoeboid, 15 μm maximal, scattered	polygonal, 20 μm maximal, many	polygonal, 20 μm maximal, many	small amoeboid /small polygonal, less than 10 μm, a few	small amoeboid /small polygonal, less than 10 μm, a few	small amoeboid /small polygonal, less than 10 μm, a few	small amoeboid /small polygonal, less than 10 μm, few
Corpus Callosum Body	small amoeboid, 15 μm maximal, scattered	amoeboid, 20 μm maximal, scattered	amoeboid, 20 μm maximal, scattered	small amoeboid /small polygonal, less than 10 μm, a few	small amoeboid /small polygonal, less than 10 μm, a few	small amoeboid /small polygonal, less than 10 μm, few	small amoeboid /small polygonal, less than 10 μm, few
Splenium <dorsal>		polygonal, 20 μm maximal, many					
Splenium <ventral>		polygonal, 20 μm maximal, many					
CD68							
Centrum Semiovale	amoeboid, 20 μm maximal, scattered	large amoeboid, 20 μm maximal, many	large amoeboid, 20 μm maximal, many	amoeboid, less than 10 μm, a few	amoeboid, less than 10 μm, a few	small amoeboid, less than 10 μm, a few	small amoeboid, less than 10 μm, a few
Corpus Callosum Body	amoeboid, 20 μm maximal, scattered	large amoeboid, 20 μm maximal, many	large amoeboid, 20 μm maximal, many	amoeboid, less than 10 μm, a few	amoeboid, less than 10 μm, a few	small amoeboid, less than 10 μm, a few	small amoeboid, less than 10 μm, a few
Splenium <dorsal>		large amoeboid, 20 μm maximal, many					
Splenium <ventral>		amoeboid, 20 μm maximal, a few					

Histological and semiquantitative evaluation of Iba-1, CD163 or CD 68 immunopositive microglia of all the patients. The numbers indicate diameters of the cytoplasm of microglia.

agenesis of corpus callosum [51].

In the present investigation, the morphology of microglia had changed even at Stage I, such as the size of microglia being larger, in the corpus callosum body than in the centrum semiovale at this stage. Morphological alteration of microglia was maximal at Stage II, corresponding to the severe degeneration and/or regeneration of axons and other cell components in the lesions at this point in the brains of ALSP. Microglia with immunopositive for Iba-1 and CD163 in the corpus callosum body at Stages II and III differed from those in the centrum semiovale. Microglia in the centrum semiovale had larger cytoplasm but evident cell processes were absent. These findings suggested that the features and intensity of the microglial reaction in the corpus callosum differed from those in the centrum semiovale, and that the process of axonal degeneration/regeneration also differed between the two. Earlier and more evident atrophy of the corpus callosum as compared with that of the centrum semiovale was considered to be caused by different reaction of microglia at the corpus callosum from that of the centrum semiovale and by decrease of commissural fibers and compaction of the remaining fibers in the present study. In addition, the size and density of spheroids were maximal at Stage II in both the centrum semiovale and the body of corpus callosum; and spheroids were larger in the corpus callosum body than in the centrum semiovale at this stage, corresponding to the degree of activation of microglia in these regions. Thus spheroids may be formed in relation to the activation of the microglia.

On the other hand, the morphology and density of microglia in the dorsal half of the splenium, representing the “focal lesions” evident on MRI [27,30,33–35], and the ventral half in patient #2 at Stage II, differed, suggesting a difference in the features and intensity of the microglial reaction in these areas. The similarity in the morphology and density of microglia in the dorsal lesion and centrum semiovale indicates that the “focal lesions” revealed by MRI developed from those in the centrum semiovale, since the dorsal part of the splenium connects the corpus callosum to the centrum semiovale via commissural fibers [52,53]. The difference in the location of “focal lesions” revealed by MRI

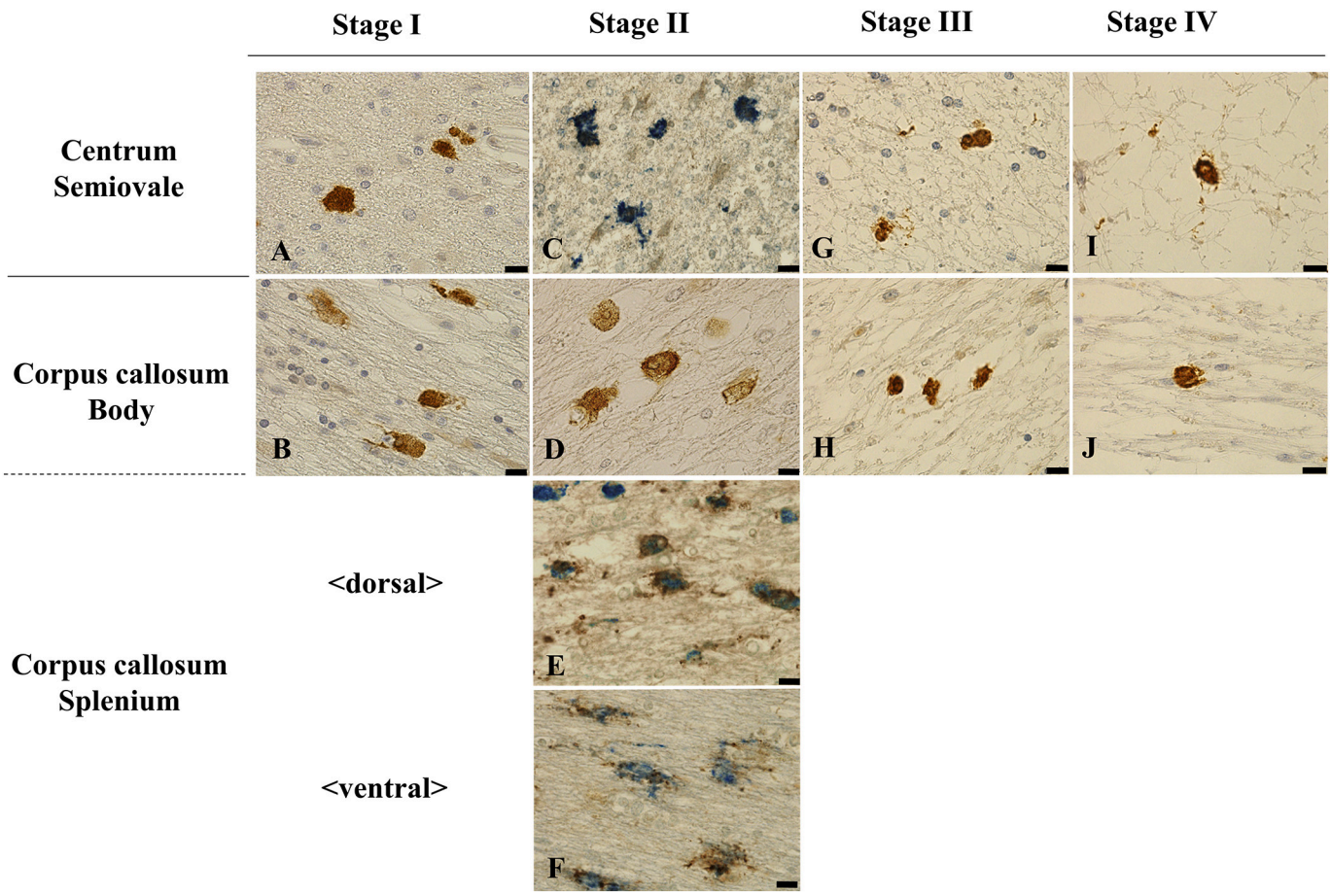

Fig. 5. CD163-immunopositive microglial cells.
Amoeboid cells with a maximal cytoplasmic diameter of 15 μm and a few short processes were scattered in both the corpus callosum (A) and centrum semiovale (B) at Stage I. Polygonal cells with a maximal diameter of 20 μm with several thick short processes were abundant in the centrum semiovale (C) and dorsal (E) and ventral (F) parts of the splenium in Patient #2, but oval amoeboid cells with a maximal diameter of 20 μm were scattered in the body of the corpus callosum (D) at Stage II. A few small oval or polygonal cells less than 10 μm in diameter with sparse processes were seen in the centrum semiovale and body of the corpus callosum at Stages III and IV (G, H, I, J). Immunohistochemistry for CD163 (brown) (A, B, D, and G - J), and double immunohistochemistry for CD163 (blue) and Iba1 (brown) (C, E, F). Bars; 10 μm. (For interpretation of the references to colour in this figure legend, the reader is referred to the web version of this article.)

among patients with ALSP reported may be due to different localization of involved areas in the centrum semiovale.

Microglial activation appeared to subside through Stages III and IV, whereas depletion of axons and disappearance of spheroids advanced in the corpus callosum, together with hollowing of the centrum semiovale. The pathological mechanism responsible for this remains unknown, and the mechanism responsible for sparing of U-fibers around the hollows at the Stages III and IV is also unclear. The forefront of the lesions extended to the brainstem, cerebellum, optic nerve and spinal cord at Stages III and IV.

Specific responses and alteration of the microglia occurring in the corpus callosum in various pathologic conditions [49–51] may indicate a possibility of particular alteration of microglia and preferential thinning of the corpus callosum in ALSP. However, there have been no reports on the expression of CSF1R, nor on the structure and amount of the CSF1R protein for each site and each cell type. Further study should be performed on these points in relation to the particular response of the microglia and the preferential thinning of the corpus callosum.

In conclusion, the present study confirmed that axonal loss advances in the body of the corpus callosum with lesion staging in patients with ALSP, as in the centrum semiovale, but that the microglial reaction in the former differs from that in latter, especially at Stages II and III. Spheroids in the body of the corpus callosum are larger than those in the centrum semiovale at Stage II. The preferential thinning of corpus callosum was considered to be formed in relation to peculiar morphological alteration of microglia there in ALSP, instead, the “focal corpus callosum lesions” revealed by MRI in patients with ALSP are formed in connection with the lesions in the centrum semiovale.

Funding

This work was supported in part by the Japan Society for the Promotion of Science (JSPS) grant-in-aid for scientific research No. 19K07820 and the Collaborative Research Project (No 201913) of Brain Research Institute, Niigata University, Japan to K. Oyanagi, AMED, Japan, under grant no. JP18dm0107105, 19dm0107105, and JP16kk0205009 to M. Yoshida, and grants-in-aid from the Research Committee of CNS Degenerative Diseases, Research on Policy Planning and Evaluation for Rare and Intractable Diseases, Health, Labor and Welfare Sciences Research Grants, the Ministry of Health, Labor and Welfare, Japan to M. Yoshida.

Ethical approval

This study was approved by the Ethics Committee of Shinshu University, Japan (No. 4415).

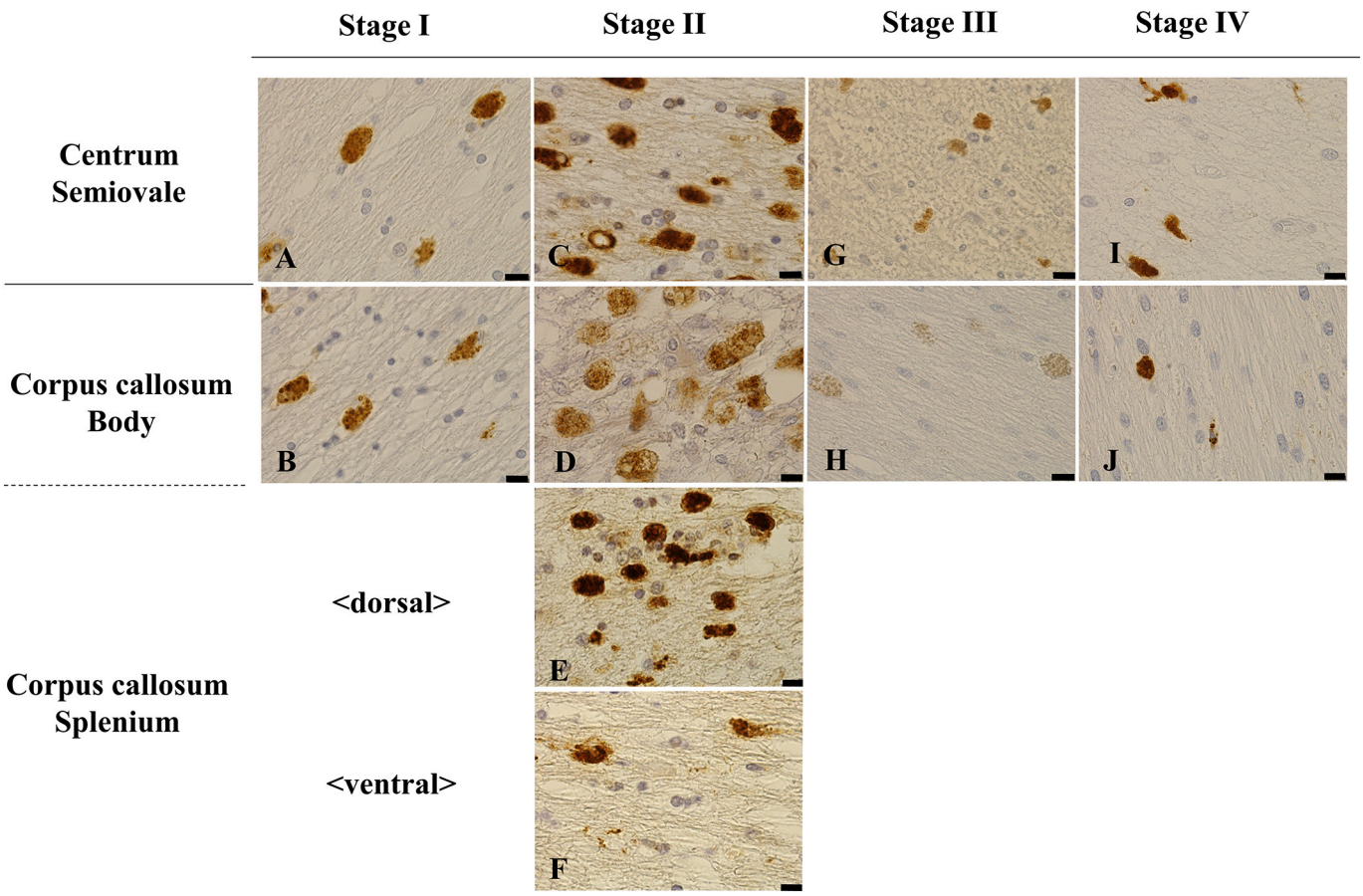

Fig. 6. CD 68-immunopositive microglial cells.
Oval-shaped amoeboid cells with a maximal diameter of 20 μm were scattered in both the centrum semiovale (A) and corpus callosum body (B) at Stage I. Many were present in the centrum semiovale (C), the body level (D) and dorsal part of the splenium of the corpus callosum in Patient #2corresponding to the "focal lesions" revealed by MRI (E), but few were evident in the ventral part of the splenium (F) at Stage II. However, a few cells less than 10 μm in diameter were seen in the centrum semiovale and body of the corpus callosum at Stages III and IV (G - J). CD68 immunohistochemistry (brown). Bars; 10 μm. (For interpretation of the references to colour in this figure legend, the reader is referred to the web version of this article.)

Informed consent

Informed consent was obtained from all individual patients and control subjects included in the present study.

Credit author statement

M Kinoshita, K Oyanagi; plannig and organizing the research, K Ishizawa, K Ishihara, M Yoshida, T Inoue, Y Mitsuyama, Y Sekijima, S Ikeda, Y Kondo; providing cases examined and analysis of the clinical data, K Yoshida; genetic analysis, M Yamada; immunohistochemistry. The corresponding author is responsible for ensuring that the descriptions are accurate and agreed by all authors.

Declaration of Competing Interest

The authors state that they have no Conflict of Interest (COI).

Acknowledgements

The authors thank Ms. Mika Tokiwai and Ms. Emi Suzuki-Kouyama (Division of Neuropathology, Department of Brain Disease Research, Shinshu University School of Medicine, Matsumoto, Japan) for their technical assistance in the immunohistochemistory.

References

[1] K. Oyanagi, M. Kinoshita, E. Suzuki-Kouyama, T. Inoue, A. Nakahara, M. Tokiwai, et al., Adult onset leukoencephalopathy with axonal spheroids and pigmented glia (ALSP) and Nasu-Hakola disease: lesion staging and dynamic changes of axons and microglical subsets, Brain Pathol 27 (2017) 748–769, https://doi.org/10.1111/bpa.12443.

[2] R. Axelsson, M. Röyttä, P. Sourander, H.O. Akesson, O. Andersen, Hereditary diffuse leukoencephalopathy with spheroids, Acta Psychiatr Scand (Suppul) 314 (1984) 1–65.

[3] Y. Baba, B. Ghetti, M.C. Baker, R.J. Uitti, M.L. Hutton, K.K. Yamaguchi, et al., Hereditary diffuse leukoencephalopathy with spheroids: clinical, pathologic and genetic studies of a new kindred, Acta Neuropathol 111 (2006) 300–311, https://doi.org/10.1007/s00401-006-0046-z.

[4] S.H. Freeman, B.T. Hyman, K.B. Sims, E.T. Hedley-Whyte, A. Vossough, M. P. Frosch, et al., Adult onset leukodystrophy with neuroaxonal spheroids: clinical, neuroimaging and neuropathologic observations, Brain Pathol 19 (2009) 39–47, https://doi.org/10.1111/j.1750-3639.2008.00163.x.

[5] K. Itoh, K. Shiga, K. Shimizu, M. Muranishi, M. Nakagawa, S. Fushiki, Autosomal dominant leukodystrophy with axonal spheroids and pigmented glia: clinical and neuropathological characteristics, Acta Neuropathol 111 (2006) 39–45, https://doi.org/10.1007/s00401-005-1113-6.

[6] M. Kinoshita, K. Yoshida, K. Oyanagi, T. Hashimoto, S. Ikeda, Hereditary diffuse leukoencephalopathy with spheroids caused by R782H mutation in *CSF1R*: case report, J Neurol Sci 318 (2012) 115–118, https://doi.org/10.1016/j.jns.2012.03.012.

[7] K. Kleinfeld, B. Mobley, P. Hedera, A. Wegner, S. Sriram, S. Pawate, et al., Adult-onset leukoencephalopathy with neuroaxonal spheroids and pigmented glia: report of five cases and a new mutation, J Neurol 260 (2013) 558–571, https://doi.org/10.1007/s00415-012-6680-6.

[8] T. Konno, M. Tada, M. Tada, A. Koyama, H. Nozaki, Y. Harigaya, et al., Haploinsufficiency of *CSF-1R* and clinicopathologic characterization in patients with HDLS, Neurology 82 (2014) 139–148, https://doi.org/10.1212/WNL.0000000000000046.

[9] J.D. Marotti, S. Tobias, J.D. Fratkin, J.M. Powers, C.H. Rhodes, Adult onset leukodystrophy with neuroaxonal spheroids and pigmented glia: report of a family, historical perspective, and review of the literature, Acta Neuropathol 107 (2004) 481–488, https://doi.org/10.1007/s00401-004-0847-x.
[10] J. Mitsui, T. Matsukawa, H. Ishiura, K. Higasa, J. Yoshimura, T.L. Saito, et al., *CSF1R* mutations identified in three families with autosomal dominantly inherited leukoencephalopathy, Am J Med Genet B Neuropsychiatr Genet 57 (2012) 951–957, https://doi.org/10.1002/ajmg.b.32100.
[11] A.M. Nicholson, M.C. Baker, N.A. Finch, C. Wider, N.R. Graff-Radford, et al., *CSF1R* mutations link POLD and HDLS as a single disease entity, Neurology 80 (2013) 1033–1040, https://doi.org/10.1212/WNL.0b013e31828726a7.
[12] C. Sundal, J.A. Van Gerpen, A.M. Nicholson, C. Wider, E.A. Shuster, J. Aasly, et al., MRI characteristics and scoring in HDLS due to *CSF1R* gene mutation, Neurology 79 (2012) 566–574, https://doi.org/10.1212/WNL.0b013e318263575a.
[13] S. Terada, H. Ishizu, O. Yokota, T. Ishihara, H. Nakashima, A. Kugo, et al., An autopsy case of hereditary diffuse leukoencephalopathy with spheroids, clinically suspected of Alzheimer's disease, Acta Neuropathol 108 (2004) 538–545, https://doi.org/10.1007/s00401-004-0920-5.
[14] M.S. van der Knaap, S. Naidu, B.K. Kleinschmidt-Demasters, W. Kamphorst, H. C. Weinstein, Autosomal dominant diffuse leukoencephalopathy with neuroaxonal spheroids, Neurology 54 (2000) 463–468, https://doi.org/10.1212/wnl.54.2.463.
[15] C. Wider, J.A. Van Gerpen, S. DeArmond, E.A. Shuster, D.W. Dickson, Z. K. Wszolek, Leukoencephalopathy with spheroids (HDLS) and pigmentary leukodystrophy (POLD): a single entity? Neurology 72 (2009) 1953–1959, https://doi.org/10.1212/WNL.0b013e3181a826c0.
[16] T. Miura, N. Mezaki, T. Konno, A. Iwasaki, N. Hara, M. Miura, et al., Identification and functional characterization of novel mutations including frameshift mutation in exon 4 of *CSF1R* in patients with adult-onset leukoencephalopathy with axonal spheroids and pigmented glia, J Neurol 265 (2018) 2415–2424, https://doi.org/10.1007/s00415-018-9017-2.
[17] C. Pridans, K.A. Sauter, K. Baer, H. Kissel, D.A. Hume, *CSF1R* mutations in hereditary diffuse leukoencephalopathy with spheroids are loss of function, Sci Rep 3 (2013) 3013, https://doi.org/10.1038/srep03013.
[18] R. Rademakers, M. Baker, A.M. Nicholson, N.J. Rutherford, N. Finch, A. Soto-Ortolaza, et al., Mutations in the colony stimulating factor 1 receptor (*CSF1R*) gene cause hereditary diffuse leukoencephalopathy with spheroids, Nat Genet 44 (2012) 200–205, https://doi.org/10.1038/ng.1027.
[19] R. Lakshmanan, M.E. Adams, D.S. Lynch, J.A. Kinsella, R. Phadke, J.M. Schott, et al., Redefining the phenotype of ALSP and *AARS2* mutation-related leukodystrophy, Neurol Genet 3 (2017), e135, https://doi.org/10.1212/NXG.0000000000000135.
[20] D.S. Lynch, W.J. Zhang, R. Lakshmanan, J.A. Kinsella, G.A. Uzun, M. Karbay, et al., Analysis of mutations in *AARS2* in a series of *CSF1R*-negative patients with adult-onset leukoencephalopathy with axonal spheroids and pigmented glia, JAMA Neurol 73 (2016) 1433–1439, https://doi.org/10.1001/jamaneurol.2016.2229.
[21] I. Taglia, I. Di Donato, S. Bianchi, A. Cerase, L. Monti, R. Marconi, et al., *AARS2*-related ovarioleukodystrophy: clinical and neuroimaging features of three new cases, Acta Neurol Scand 138 (2018) 278–283, https://doi.org/10.1111/ane.12954.
[22] D. Wang, M. Yu, W. Zhang, Z. Wang, Y. Yuan, *AARS2* compound heterozygous variants in a case of adult-onset leukoencephalopathy with axonal spheroids and pigmented glia, J Neuropathol Exp Neurol 77 (2018) 997–1000, https://doi.org/10.1093/jnen/nly087.
[23] H. Akiyama, T. Nishimura, H. Kondo, K. Ikeda, Y. Hayashi, P.L. McGeer, Expression of the brain microglia and its upregulation in brains of patients with Alzheimer's disease and amyotrophic lateral sclerosis, Brain Res 639 (1994) 171–174, https://doi.org/10.1016/0006-8993(94)91779-5.
[24] Y. Riku, T. Ando, Y. Goto, K. Mano, Y. Iwasaki, G. Sobue, M. Yoshida, Early pathologic changes in hereditary diffuse leukoencephalopathy with spheroids, J. Neuropathol. Exp. Neurol 73 (2014) 1183–1190, https://doi.org/10.1097/NEN.0000000000000139.
[25] M. Tada, T. Konno, M. Tada, T. Tezuka, T. Miura, N. Mezaki, et al., Characteristic microglial features in patients with hereditary diffuse leukoencephalopathy with spheroids, Ann Neurol 80 (2016) 554–565, https://doi.org/10.1002/ana.24754.
[26] M. Kinoshita, Y. Kondo, K. Yoshida, K. Fukushima, K. Hoshi, K. Ishizawa, et al., Corpus callosum atrophy in patients with hereditary diffuse leukoencephalopathy with neuroaxonal spheroids: an MRI-based study, Intern Med 53 (2014) 21–27, https://doi.org/10.2169/internalmedicine.53.0863.
[27] Y. Kondo, M. Kinoshita, K. Fukushima, K. Yoshida, S. Ikeda, Early involvement of the corpus callosum in a patient with hereditary diffuse leukoencephalopathy with spheroids carrying the *de novo* K793T mutation of *CSF1R*, Intern Med 52 (2013) 503–506, https://doi.org/10.2169/internalmedicine.52.8879.
[28] Y. Kondo, A. Matsushima, S. Nagasaki, K. Nakamura, Y. Sekijima, K. Yoshida, Factors predictive of the presence of a *CSF1R* mutation in patients with leukoencephalopathy, Eur J Neurol 27 (2020) 369–375, https://doi.org/10.1111/ene.14086.
[29] T. Konno, K. Yoshida, T. Mizuno, T. Kawarai, M. Tada, H. Nozaki, et al., Clinical and genetic characterization of adult-onset leukoencephalopathy with axonal spheroids and pigmented glia associated with *CSF1R* mutation, Eur J Neurol 24 (2017) 37–45, https://doi.org/10.1111/ene.13125.
[30] T. Konno, K. Yoshida, I. Mizuta, T. Mizuno, T. Kawarai, M. Tada, et al., Diagnostic criteria for adult-onset leukoencephalopathy with axonal spheroids and pigmented glia due to *CSF1R* mutation, Eur J Neurol 25 (2018) 142–147, https://doi.org/10.1111/ene.13464.
[31] F.F. Figueira, V.S. Santos, G.M. Figueira, A.C. Silva, Corpus callosum index: a practical method for long-term follow-up in multiple sclerosis, Arq Neuropsiquiatr 65 (2007) 931–935, https://doi.org/10.1590/s0004-282x2007000600001.
[32] O. Yaldizli, R. Atefy, A. Gass, D. Sturm, S. Glassl, B. Tettenborn, et al., Corpus callosum index and long-term disability in multiple sclerosis patients, J Neurol 257 (2010) 1256–1264, https://doi.org/10.1007/s00415-010-5503-x.
[33] S.J. Adams, A. Kirk, R.N. Auer, Adult-o nset leukoencephalopathy with axonal spheroids and pigmented glia (ALSP): integrating the literature on hereditary diffuse leukoencephalopathy with spheroids (HDLS) and pigmentary orthochromatic leukodystrophy (POLD), J Clin Neurosci 48 (2018) 42–49, https://doi.org/10.1016/j.jocn.2017.10.060.
[34] B. Saitoh, R. Yamasaki, S. Hayashi, S. Yoshimura, T. Tateishi, Y. Ohyagi, et al., A case of hereditary diffuse leukoencephalopathy with axonal spheroids caused by a de novo mutation in *CSF1R* masquerading as primary progressive multiple sclerosis, Mult Scler 19 (2013) 1367–1370, https://doi.org/10.1177/1352458513489853.
[35] B. Saitoh, R. Yamasaki, A. Hiwatashi, T. Matsushita, S. Hayashi, Y. Mitsunaga, et al., Discriminative clinical and neuroimaging features of motor-predominant hereditary diffuse leukoencephalopathy with axonal spheroids and primary progressive multiple sclerosis: a preliminary cross-sectional study, Mult Scler Relat Disord 31 (2019) 22–31, https://doi.org/10.1016/j.msard.2019.03.008.
[36] K. Ishihara, Y. Horibe, H. Ohno, M. Sugie, J. Shiota, I. Nakano, et al., A clinicopathological study of young-onset dementia: report of 2 autopsied cases, Brain Nerve 63 (2011) 1117–1123 (Article in Japanese).
[37] T. Kimura, K. Ishizawa, T. Mitsufuji, T. Abe, Y. Nakazato, K. Yoshida, et al., A clinicopathological and genetic study of sporadic diffuse leukoencephalopathy with spheroids: a report of two cases, Neuropathol Appl Neurobiol 39 (2013) 837–843, https://doi.org/10.1111/nan.12046.
[38] Y. Kondo, M. Kinoshita, T. Yoshida, H. Matoba, T. Uehara, M. Ikeyama, et al., Unexpected occurrence of Fetal Hemophagocytic syndrome in a patient with hereditary diffuse leukoencephalopathy with spheroids, Case Rep Clin Med 5 (2016) 77–84, https://doi.org/10.4236/crcm.2016.53014.
[39] G. Sulter, C. Steen, J. De Keyser, Use of the Barthel index and modified Rankin scale in acute stroke trials, Stroke 30 (1999) 1538–1541, https://doi.org/10.1161/01.str.30.8.1538.
[40] Z. Ahmed, G. Shaw, V.P. Sharma, C. Yang, E. McGowan, D.W. Dickson, Actin-binding proteins coronin-1a and IBA-1 are effective microglial markers for immunohistochemistry, J Histochem Cytochem 55 (2017) 687–700, https://doi.org/10.1369/jhc.6A7156.2007.
[41] D. Ito, Y. Imai, K. Ohsawa, K. Nakajima, Y. Fukuuchi, S. Kohsaka, Microglia-specific localization of a novel calcium binding protein, Iba1. Mol Brain Res 57 (1998) 1–9, https://doi.org/10.1016/S0169-328X(98)00040-0.
[42] K.M. Murphy, Janeway's Immunobiology, eighth ed., Garland Science, New York, 2012.
[43] A. Etzerodt, S.K. Moestrup, CD163 and inflammation: biological diagnostic, and therapeutic aspects, Antioxid Redox Signal 18 (2013) 2352–2363, https://doi.org/10.1089/ars.2012.4834.
[44] E.E. Benarroch, Microglia: multiple roles in surveillance, circuit shaping, and response to injury, Neurology 81 (2013) 1079–1088, https://doi.org/10.1212/WNL.0b013e3182a4a577.
[45] Y. Imai, S. Kohsaka, Intracellular signaling in M-CSF-induced microglia activation: role of Iba1, Glia 40 (2002) 164–174, https://doi.org/10.1002/glia.10149.
[46] V. Chitu, E.R. Stanley, Regulation of embryonic and postnatal development by the CSF-1 receptor, Curr Top Dev Biol 123 (2017) 229–275, https://doi.org/10.1016/bs.ctdb.2016.10.004.
[47] T. Mizuno, Y. Doi, H. Mizoguchi, S. Jin, M. Noda, Y. Sonobe, et al., Interleukin-34 selectively enhances the neuroprotective effects of microglia to attenuate oligomeric amyloid-β neurotoxicity, Am J Pathol 179 (2011) 2016–2027, https://doi.org/10.1016/j.ajpath.2011.06.011.
[48] A. Suzumura, Microglia in neurodegenerative disorders and neuroinflammation, Clin. Neurol 54 (2014) 1119–1121 (Article in Japanese), https://doi.org/10.5692/clinicalneurol.54.1119.
[49] J.M. Hillis, J. Davies, M.V. Mundim, O. Al-Dalahmah, F.G. Szele, Cuprizone demyelination induces a unique inflammatory response in the subventricular zone, J Neuroinflammation 13 (2016) 190, https://doi.org/10.1186/s12974-016-0651-2.
[50] V. Chitu, S. Gokhan, M. Gulinello, C.A. Branch, M. Patil, R. Basu, et al., Phenotypic characterization of a *Csf1r* haploinsufficient mouse model of adult-onset leukodystrophy with axonal spheroids and pigmented glia (ALSP), Neurobiol Dis 74 (2015) 219–228, https://doi.org/10.1016/j.nbd.2014.12.001.
[51] N. Oosterhof, I.J. Chang, E.G. Karimiani, I.E. Kuil, D.M. Jensen, R. Daza, et al., Homozygous mutations in *CSF1R* cause a Pediatric-onset leukoencephalopathy and can result in congenital absence of microglia, Am J Hum Genet 104 (2019) 936–947, https://doi.org/10.1016/j.ajhg.2019.03.010.
[52] M.C. de Lacoste, J.B. Kirkpatrick, E.D. Ross, Topography of the human corpus callosum, J Neuropathol Exp Neurol 44 (1985) 578–591.
[53] M.G. Knyazeva, Splenium of corpus callosum: patterns of interhemispheric interaction in children and adults, Neural Plast 2013 (2013) 639430, https://doi.org/10.1155/2013/639430.
[54] J. Paloneva, M. Kestilä, J. Wu, A. Salminen, T. Böhling, V. Ruotsalainen, et al., Loss-of-function mutations in *TYROBP* (*DAP12*) result in a presenile dementia with bone cysts, Nat Genet 25 (2000) 357–361, https://doi.org/10.1038/77153.
[55] J. Paloneva, T. Manninen, G. Christman, K. Hovanes, J. Mandelin, R. Adolfsson, et al., Mutations in two genes encoding different subunits of a receptor signaling complex result in an identical disease phenotype, Am J Hum Genet 71 (2002) 656–662, https://doi.org/10.1086/342259.